

Biocompatible Polysiloxane-Containing Diblock Copolymer PEO-*b*-P γ MPS for Coating Magnetic Nanoparticles

Hongwei Chen,[†] Xinying Wu,^{†,‡} Hongwei Duan,[§] Y. Andrew Wang,^{||} Liya Wang,[†] Minming Zhang,[‡] and Hui Mao^{*,†}

Department of Radiology, Center for Systems Imaging and Center for MR Research, Emory University School of Medicine, Atlanta, Georgia 30322, Department of Radiology, Zhejiang University School of Medicine, Hangzhou, Zhejiang, China, Wallace Coulter Department of Biomedical Engineering, Emory University and Georgia Institute of Technology, Atlanta, Georgia 30322, and Ocean NanoTech, LLC, 2143 Worth Lane, Springdale, Arkansas 72701

ABSTRACT We report a biocompatible polysiloxane containing amphiphilic diblock copolymer, poly(ethylene oxide)-*block*-poly(γ -methacryloxypropyltrimethoxysilane) (PEO-*b*-P γ MPS), for coating and stabilizing nanoparticles for biomedical applications. Such an amphiphilic diblock copolymer that comprises both a hydrophobic segment with “surface anchoring moiety” (silane group) and a hydrophilic segment with PEO ($M_n = 5000$ g/mol) was obtained by the reversible addition–fragmentation chain transfer (RAFT) polymerization using the PEO macromolecular chain transfer agent. When used for coating paramagnetic iron oxide nanoparticles (IONPs), copolymers were mixed with hydrophobic oleic acid coated core size uniformed IONPs ($D = 13$ nm) in cosolvent tetrahydrofuran. After being aged over a period of time, resulting monodispersed IONPs can be transferred into aqueous medium. With proper P γ MPS block length ($M_n = 10\,000$ g/mol), polysiloxane containing diblock copolymers formed a thin layer of coating (~ 3 nm) around monocrystalline nanoparticles as measured by transmission electron microscopy (TEM). Magnetic resonance imaging (MRI) experiments showed excellent T_2 weighted contrast effect from coated IONPs with a transverse relaxivity $r_2 = 98.6$ mM⁻¹ s⁻¹ (at 1.5 T). Such thin coating layer has little effect on the relaxivity when compared to that of IONPs coated with conventional amphiphilic copolymer. Polysiloxane containing diblock copolymer coated IONPs are stable without aggregation or binding to proteins in serum when incubated for 24 h in culture medium containing 10% serum. Furthermore, a much lower level of intracellular uptake by macrophage cells was observed with polysiloxane containing diblock copolymers coated IONPs, suggesting the reduction of nonspecific cell uptakes and antibiofouling effect.

KEYWORDS: diblock copolymer • silanes • coating • nanoparticle • magnetic resonance imaging

INTRODUCTION

Surface coating materials play important roles in developing nanomaterials for biological and medical applications. Proper coating materials can provide biocompatibility, safety, surface functionalization that is required for specific in vitro and in vivo applications. For in vivo applications of nanoparticles, high nonspecific uptake of nanoparticles by the reticuloendothelial system (RES)¹ is recognized as one of the great challenges (1). However, such nonspecific RES uptake may be altered or controlled by modulating the properties of coating polymers (2, 3). Fur-

thermore, nanoparticles such as magnetic iron oxide nanoparticles (IONP) made using methods with nonaqueous conditions often provide high qualities and more uniformed physicochemical properties than those made in aqueous medium (4, 5). Such hydrophobic nanoparticles usually have to be transferred into water or other aqueous medium in most biomedical applications. This can be achieved by applying for specific designed polymer coating that provides a core–shell structure with a hydrophobic inner layer stabilize nanoparticles but a hydrophilic outer layer to make nanoparticles uniformly dispersed in water (6). Recently, silanes have become increasingly attractive for coating nanoparticles, such as IONPs (7–10). Silanol groups provide ideal hydrophilic water-polymer interface, allowing for coated nanoparticles stabilized in aqueous and physiological medium. To derivatize and functionalize the nanoparticle surface, silanol groups are readily available for reacting with a variety of functional groups through the rich chemistry of siloxane-based molecules. Therefore, there is a range of possibilities to conjugate targeting and affinity ligands for biomarker detections or introduce payload molecules for nanoparticle-based delivery.

Two methods have been reported for coating IONPs with silica materials: i.e., acidic hydrolysis of silica in aqueous

* Corresponding author. Phone: (404) 712-0357. Fax: (404) 712-5948. E-mail: hmao@emory.edu.

Received for review April 18, 2009 and accepted July 17, 2009

[†] Emory University School of Medicine.

[‡] Zhejiang University School of Medicine.

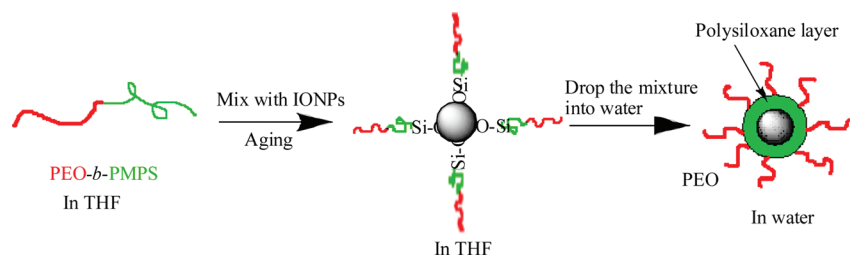
[§] Emory University and Georgia Institute of Technology.

^{||} Ocean NanoTech.

¹ Abbreviations: PEO, poly(ethylene oxide); P γ MPS, poly(γ -methacryloxypropyltrimethoxysilane); DLS, dynamic light scattering; MRI, magnetic resonance imaging; NMR, nuclear magnetic resonance; GPC, gel permeation chromatography; IONPs, iron oxide nanoparticles; TEOS, tetraethylorthosilicate; RAFT, reversible addition–fragmentation chain transfer; TEM, transmission electron microscopy; FBS, fetal bovine serum; RES, reticular endothelial system.

DOI: 10.1021/am900262j

© 2009 American Chemical Society

Scheme 1. Schematic Illustration of Polysiloxane Coated IONP Using Block Copolymer PEO-*b*-P γ MPS

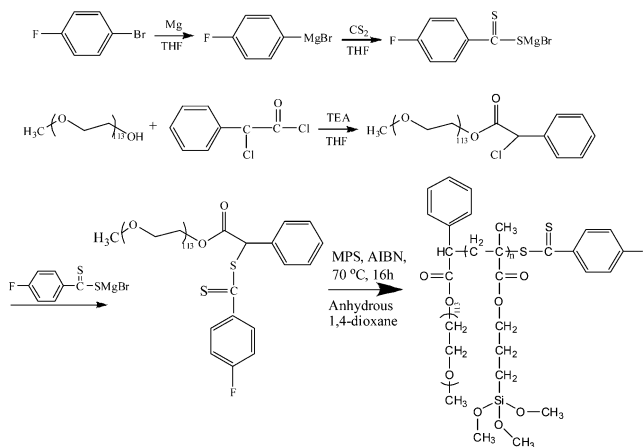
solutions (11) and a modified Stöber process (12), in which silica was formed in situ through the hydrolysis and condensation of a sol-gel precursor, such as tetraethylorthosilicate (TEOS). Deposition of silica from silicate solution usually yields relatively big and less uniformed particles with a mean size in the range of 80–200 nm (13). However, these particles are useful for in vitro biomolecule separation or sensing but can not be readily used for in vivo applications with intravenous delivery. It was shown that silica-coated IONPs with the mean diameter of 60–120 nm can be obtained by the Stöber process from initial 5–15 nm size Fe₃O₄ precursors only after the bare magnetic particles were pretreated with a small amount of silicate in an aqueous solution (14). It was also shown that the concentration of pretreated magnetite particles should be less than 12 mg/L, otherwise large aggregates of magnetite are formed in TEOS solutions (14). Further detailed studies of silica coating IONPs using TEOS (15, 16) revealed that this process is highly sensitive to experimental conditions such as ethanol/water ratio, concentration of ammonia and TEOS, and temperature, etc. To improve the homogeneity of silica-coated IONPs and to increase the concentration limits of IONPs in reaction medium, we used a modified Stöber process in reverse microemulsion conditions (17), but this method requires a large amount of surfactants associated with the microemulsion system.

Here we report a polysiloxane containing diblock copolymer: poly(ethylene oxide)-*block*-poly(γ -methacryloxypropyl trimethoxysilane) (PEO-*b*-P γ MPS) that can be used to transform and stabilize high-quality IONPs made in hydrophobic or organic medium into aqueous medium. This copolymer is soluble in organic solvent, such as tetrahydrofuran (THF), and self-assembles into micelles in water. Reactive trimethoxysilane groups in one segment can “anchor” on the surface of IONPs through ligand exchange (18) and form a polysiloxane-coated layer on IONPs. The stabilized monodispersed polysiloxane coated IONPs can be formed and stabilized through collapsing of hydrophobic block P γ MPS on the surface of IONPs and hydrophilic protection with PEO in water as shown in the Scheme 1. Resulting polysiloxane coated IONPs exhibit an excellent transverse T_2 relaxivity for MRI contrast and reduced nonspecific cell uptake for the effect of antibiofouling.

EXPERIMENTAL SECTION

Materials. γ -Methacryl oxypropyltrimethoxysilane (γ MPS) (98%, Aldrich) was purified by distillation under reduced pressure. 2,2-Azobis(isobutyronitrile) (AIBN, 98%, Aldrich) used as

Scheme 2. Synthetic Pathway for Formation of the Poly(ethylene oxide)-Based Macromolecular Chain Transfer Agent



an initiator was purified by recrystallization in ethanol. Carbon disulfide (99.9%), magnesium turnings (>99.5%), 2-chloro-2-phenylacetyl chloride (CPAC, 90%), poly(ethylene oxide) monomethyl ether (PEO) ($M_n = 5000$ g/mol, $M_w/M_n = 1.10$), anhydrous dioxane (99.8%), anhydrous tetrahydrofuran (THF, 99.8%) and all other chemicals were purchased from Aldrich and used as received. PEO has long been recognized as a biocompatible material and can be soluble in both organic and aqueous media. Dithioester RAFT agent that gives block formation from PEO-based macro-CTA is shown in Scheme 2, which is similar to that reported by Li et al. (19).

Preparation of IONPs. Hydrophobic iron oxide nanocrystals coated with oleic acid were prepared by heating iron oxide powder and oleic acid in octadecene over 315 °C. This process allows for obtaining small and size uniformed nanoparticles. The size of IONPs was tuned through modulating experimental conditions such as heating time, temperature, and ratio of the iron oxide and oleic acid (20). For comparing properties of established and widely used IONPs, we use the water-soluble IONPs coated with amphiphilic copolymers adopting the approach developed by Gao et al. (21) for coating quantum dots.

Synthesis of Diblock Copolymer PEO-*b*-P γ MPS. (A) Esterification of PEO with Chlorophenylacetic acid (PEO-CPA) (19). Poly(ethylene oxide) monomethyl ether (40.0 g, 8 mmol), triethylamine (TEA) (3.4 mL, 24 mmol), and 2-chloro-2-phenylacetyl chloride (2.4 mL, 16 mmol) were mixed in a round-bottom flask using anhydrous THF (150 mL) as solvent, and the solution was refluxed for 2 days at atmospheric pressure. The solvent was then removed, and 100 mL chloroform was added. The resulting solution was washed with saturated sodium bicarbonate solution three times, and the yellow organic phase was dried over anhydrous magnesium sulfate. The product was further purified by precipitation in diethyl ether. (B) Synthesis of PEO Macro-CTA. A THF solution (10 mL) of 4-fluorobromobenzene (2.2 mL, 20 mmol) was added dropwise to a mixture of Mg (0.50 g, 20 mmol) in THF (40 mL) and a crystal

of I₂ in a three-necked round-bottom flask equipped with a condenser and a magnetic stirrer with a nitrogen atmosphere. The mixture was refluxed for 3 h and then cooled to room temperature. Carbon disulfide (6.0 mL, 99 mmol) was added dropwise, and the solution was stirred for 1 h at room temperature and then heated to 40 °C for 2 h. After cooling the solution to 0 °C, 100 mL of ice water was added dropwise. Any solids were removed by centrifugation and the solution was then washed with diethyl ether four times. The purified solution (denoted as solution A) was kept in the refrigerator for use. 5.0 g of PEO-CPA was dissolved in 40 mL of water by adding 5 mL of THF to facilitate dissolving. Twenty-five milliliters of solution A was added dropwise into PEO-CPA solution with vigorous stirring at 0–10 °C for 24 h. After reaction, both 100 mL of CHCl₃ and 23 g of NaCl were added to the reaction solution to extract the resultant product into the organic phase followed by washing three times using saturated sodium bicarbonate solution. After drying over anhydrous magnesium sulfate, the resultant product was precipitated in diethyl ether to give PEO-CTA. C) Synthesis of the PEO-*b*-P γ MPS diblock copolymer. The polymerization was performed in a Schlenk flask with a magnetic stirring bar. The polymerization procedure is as follows. γ MPS (1.2 mL, 5 mmol), PEO-CTA (0.69 g, 0.12 mmol), and AIBN (7.1 mg, 0.04 mmol) were added along with anhydrous 1,4-dioxane (2 mL). The mixture was degassed and then sealed under a vacuum. The flask was then immersed into an oil bath preheated to 70 °C to start the polymerization. After 17 h, the reaction flask was quenched into the mixture of dry ice/2-propanol to stop the polymerization. Purification was carried out in an Atmosbag filled with argon. After three cycles of precipitation in petroleum ether, the polymer was dried under vacuum overnight. ¹H NMR spectra of P γ MPS block polymers were recorded in CDCl₃ using a Mercury Innova 600 MHz spectrometer. Molar mass and molar mass distributions of the PEO macro-RAFT agent and copolymer PEO-*b*-P γ MPS were determined by gel permeation chromatography (GPC) with THF as the eluent (flow rate = 1.0 mL/min). A series of four linear Styragel columns: HR0.5, HR1, HR2 and HR4 and a column temperature of 30 °C were used. An Agilent 1200 pump and differential refractive index detector were applied for detection. Near-monodisperse linear polystyrene standards were used to construct the calibration curve. The purified copolymer was dissolved in anhydrous THF to form a solution with concentration at 50 mg/mL.

Block Copolymer Stabilized IONPs. The oleic-acid-coated IONPs, which are not stable in water, were dispersed in anhydrous THF to form a 5.0 mg/mL solution. Two milliliters of such a solution was mixed with 2.0 mL of PEO-*b*-P γ MPS solution (50 mg/mL in THF). After being aged for several days, such a mixture was added dropwise into 20.0 mL of water under magnetic stirring. THF in the solution was removed by dialysis against water. The solution was first centrifuged at 6000 rpm for 10 min to remove a small amount of large aggregates. The collected supernatant was then purified by using Frantz laboratory magnetic separator. Such a wash-resuspend step was repeated three times. The final iron concentration of the IONP solution was estimated through optical absorption at 500 nm. The average hydrodynamic diameter and the size distribution of block copolymer micelles and copolymer-coated IONPs were measured using a Malvern Zeta Sizer Nano S-90 dynamic light scattering (DLS) instrument equipped with a 22 mW He-Ne laser operating at $\lambda = 632.8$ nm. The core sizes of copolymer-coated IONPs and thickness of polymer layers were viewed and measured using transmission electron microscopy (TEM) (Hitachi H-7500 instrument (75 kv)). A drop of diluted solution was put on the grid and dried in the air.

MRI Relaxativity Measurements. Magnetic resonance imaging (MRI) studies were carried out on MRI scanners at the field strengths of 1.5 T. For transverse relaxation time T_2 measure-

ments, a multiecho fast spin-echo sequence was used to simultaneously collect 20 data points at different echo times ($T_E = 6$ to 180 ms with an increment of 6 ms). The T_2 relaxation time of each nanoparticle sample was calculated by fitting the decay curve on a pixel-by-pixel basis by using a nonlinear monoexponential algorithm $M(TE) = M_0 \exp(-TE/T_2)$, where T_E is the echo time, and $M(TE)$ is the MRI signal intensity at which T_E is used.

Uptake of Nanoparticles by Macrophages. We selected macrophage (RAW 264.7) for testing nonspecific cell uptake of polymer coated nanoparticles. Macrophage cell line RAW 264.7 were maintained as an adherent culture and grown as a monolayer in a humidified incubator (95% air, 5% CO₂) at 37 °C in a Petri dish containing RPMI medium supplemented with 10% heat-inactivated fetal bovine serum (FBS). Cells were seeded into 8-well chamber slide and grew overnight. After exposed to IONPs at iron concentration of 0.2 and 0.1 mg/mL per well in Hanks solution for 2 h at 37 °C, cells were washed with PBS, then fixed with 0.5 mL of 4% paraformalin (PFA) for 20 min. Prussian blue staining was used to determine the presence of iron that was uptaken (binds) into cells. Each well of the chamber slide was filled with a 0.5 mL of a fresh mixture of 5% potassium ferrocyanide (II) trihydrate and 5% HCl solution, and incubated for 30 min. After being washed twice with distilled water, cells were counterstained with fast red solution and mounted to be observed. The result of Prussian blue staining was assessed by a light microscope.

RESULTS AND DISCUSSION

Figure 1 shows the ¹H NMR spectra of PEO-CPA, PEO Macro-CTA, and PEO-*b*-P γ MPS, respectively. In the spectrum of PEO-CPA (Figure 1A), the resonances at $\delta \approx 7.4$ ppm (peaks e and f) are ascribed to the aromatic protons of the phenyl group. The signal at $\delta \approx 5.39$ ppm (peak d) represents the proton from methine with Cl atom. The signal at $\delta \approx 4.2$ ppm (peak c) is due to methylene protons of newly formed ester groups (22). By comparing the intensity ratio at $\delta \approx 5.39$ ppm to that at $\delta \approx 3.37$ ppm (peak a), the degree of functionalization is estimated to be $\sim 95\%$. In the spectrum of PEO Macro-CTA (Figure 1B), the shift of the peak d from $\delta \approx 5.39$ to $\delta \approx 5.69$ ppm indicates the formation of PEO-CTA. Accordingly, the degree of functionalization for PEO-CTA is estimated to be $\sim 90\%$ by comparing the intensity ratio at $\delta \approx 5.69$ ppm (peak d') to that at $\delta \approx 3.37$ ppm. In the spectrum of PEO-*b*-P γ MPS (Figure 1C), formation of P γ MPS block resulted in the characteristic signals at $\delta \approx 3.89$ (peak e), 3.57 (peak h) and 0.6 ppm (peak g), respectively. By comparing intensity ratio at peaks b and h (Figure 1-C), which is ascribed to PEO and P γ MPS, respectively, the average number of repeating monomer for P γ MPS is estimated to be 40, and the copolymer is labeled with PEO5K-*b*-P γ MPS10K. Further GPC characterization and confirmation of the formation of the designed blocked polymer indicated that the expected elution peak shifted toward the higher molecular weight in the elution profile (shown in Figure 2) and the low PDI (i.e., 1.4) was obtained. Those results are in agreement with the formation of a block copolymer. It is worth noting that controlled radical polymerization using RAFT is applicable to a wide range of monomers including reactive monomer like γ MPS. Mellon et al. (23) first reported the polymerization of γ MPS by RAFT techniques. Using 2-cyanoprop-2-yl dithiobenzoate (CPDB) as chain transfer agent (CTA), block copolymers of γ MPS and

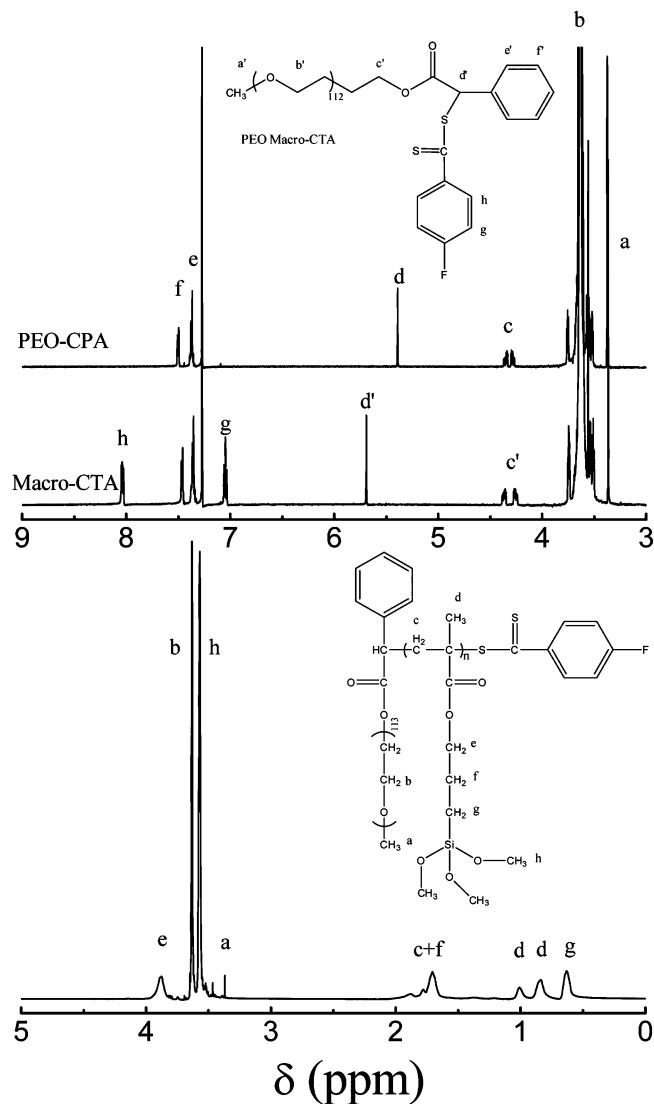


FIGURE 1. ^1H NMR spectra of (A) PEO-CPA, (B) PEO Macro-CTA, and (C) PEO-*b*- $\text{P}\gamma\text{MPS}$. Samples were dissolved in CDCl_3 .

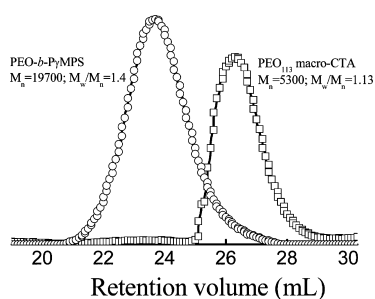


FIGURE 2. Evolution of number-average molar masses (M_n) and polydispersity indexes (PDI) obtained by GPC for PEO₁₁₃-based macromolecular chain transfer agent (PEO₁₁₃-CTA) and the corresponding chain extended copolymer PEO-*b*- $\text{P}\gamma\text{MPS}$.

MMA were successfully synthesized. The controlled $\text{P}\gamma\text{MPS}$ chains can be up to $M_n = 40\,000$ g/mol, exhibiting low polydispersity indexes (PDI < 1.3). RAFT polymerization of γMPS using PEO Macro-CTA was first and successfully carried out in this study based on the previous work (19, 23, 24).

The solution behavior of this similar block copolymer obtained through atom transfer radical polymerization (ATRP)

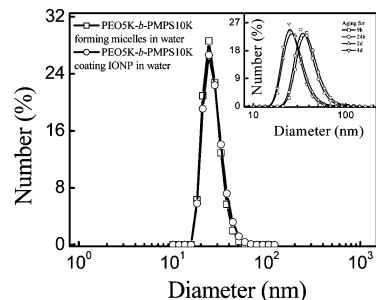


FIGURE 3. Hydrodynamic size distribution for both copolymer formed micelles and copolymer-coated IONPs in water measured by DLS. The insert shows the hydrodynamic size data at different aging time.

has been studied previously. Various self-assemblies with different morphologies have been produced by controlling the block copolymer composition, solvent property, and mixed-solvent composition (25–27). Based on the micellization behavior of this kind of copolymer, we applied this process to stable and disperse hydrophobic small molecule-coated magnetic nanoparticles in water. Figure 3 shows the size distribution and hydrodynamic sizes for both copolymer formed micelles and copolymer coated IONPs in water. Results from DLS measurements indicate that the free amphiphilic copolymer can form micelles with $D = 24$ nm. After mixing oleic acid coated hydrophobic IONPs with such copolymer in cosolvent THF followed by aging, monodispersed IONPs with copolymers replacing oleic acid coating were transferred into water. Interestingly, the size of copolymer coated IONPs remains almost the same as free copolymer micelles despite of the presence of 13 nm IONP core. It should be noted that the mixture of copolymer and IONPs in THF needs to be aged to allow copolymer completely absorbed onto the surface of IONP through ligand exchange (18). We found that the average hydrodynamic diameter of composite nanostructure decreased from 41 to 24 nm after aging 4 days as shown in the insert of Figure 3. It is worth noting that when adding hexane, in which oleic acid coated nanoparticle can stabilize well but copolymers precipitate, to the aged mixture, nanoparticles and copolymers can be coprecipitated from the solvent with copolymers forming the outer layer of IONP. Such a feature can be attributed to the fact that the polymer was absorbed on the surface of nanoparticles after aging.

Figure 4 shows the TEM images of IONPs before and after being coated with the copolymers PEO-*b*- $\text{P}\gamma\text{MPS}$. It should be noted that the IONPs used here were made via high-temperature decomposition of precursor iron oxide in the presence of oleic acid molecules. Compared with traditional IONPs synthesized by aqueous-phase chemistry, this new class of nanocrystals is highly size uniform and exhibits improved structural properties as shown in Figure 4A. Using copolymer PEO-*b*- $\text{P}\gamma\text{MPS}$ mixed with IONPs in THF allowed coated IONPs stably dispersed in water. Figure 4B shows the TEM image of IONPs mixed with copolymers through aging. A thin polymer layer can be seen around IONPs, indicating the polymer was absorbed on the surface of IONPs through ligand exchange between trimethoxysilane groups and oleic

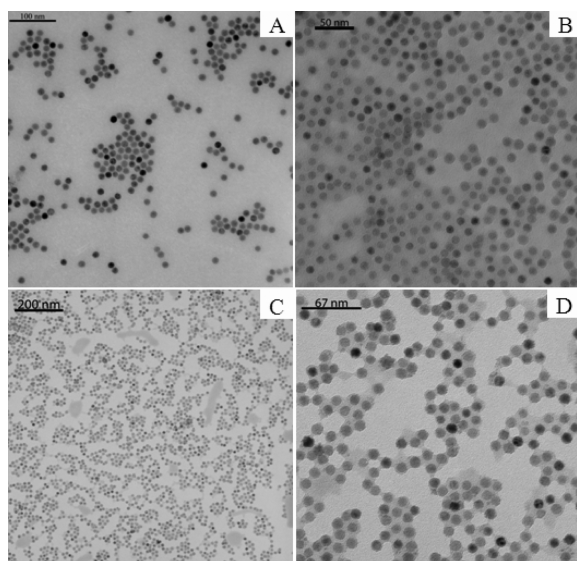


FIGURE 4. TEM images of monodispersed IONPs in (A) THF, (B) mixture of IONPs and PEO-*b*-PyMPS after aging in THF for 4 days, and (C) low- and (D) high-magnification images of PEO-*b*-PyMPS coated IONPs in water.

acid (18). Although using materials containing trimethoxysilane to coat the surface of IONPs has already been reported (18, 28), our study differs from previous studies in which small molecules were used. We use a long chain polymer containing the same “anchoring” group. Although the polymer bears reactive trimethoxysilane groups in one segment, nanoparticles in the presence of such polymer in THF are still monodispersed without aggregation or cross-linking of surface polymers. Since copolymers have “anchored” on the surface of the IONP, copolymers can directly collapse onto the surface of the IONP, while the hydrophilic block PEO prevents the further particle aggregation, copolymer coated IONPs remain monodispersed when dropping the aged mixture of copolymers and IONPs into water. Therefore, we can get composite nanostructures with single IONP as the core. Images C and D in Figure 4 show the IONPs coated with copolymer PEO-*b*-PyMPS in water. A monolayer without any large aggregates as viewed under a lower magnification indicates that such copolymer works well for coating oleic-acid-stabilized IONPs. A thin polymer layer can be seen coated around the size uniformed nanoparticles under higher magnification. Based on the measurements from TEM images, it is estimated that the thickness of the polysiloxane coating layer is about 3 nm, which is smaller than particles obtained from modified Stöber process (7, 13, 15, 29). It is worth noting that the polymer coating appears fluid, especially for PEG, even though the coating may be uniform, it still deforms on contact with the TEM grid. Another advantage of such copolymer for coating IONPs is that copolymers can self-assemble which leads to encapsulate the IONPs into micelles in water. This process has been previously described as simultaneous encapsulation method (30, 31). Although several block copolymers have been applied using this method to encapsulate the inorganic nanoparticles to make them stable in water

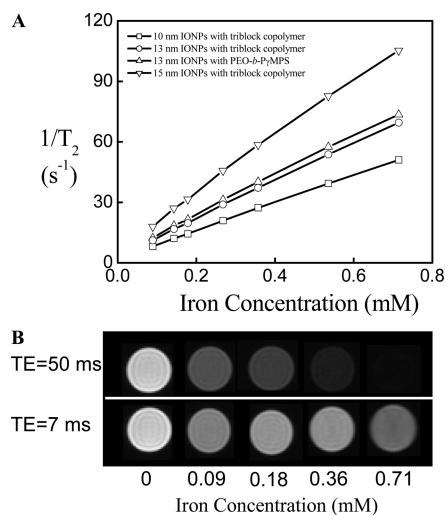


FIGURE 5. (A) T_2 relaxation rates ($1/T_2$, s^{-1}) as a function of iron concentration (mM) for polysiloxane-coated and amphiphilic copolymer-coated IONPs. (B) T_2 weighted spin echo MR images of polysiloxane coated IONPs at different concentrations showed strong contrast effect resulting from the shortening of T_2 relaxation time. T_2 weighted MRI contrast is induced by IONPs as the signal drop at longer TE (7 vs 50 ms).

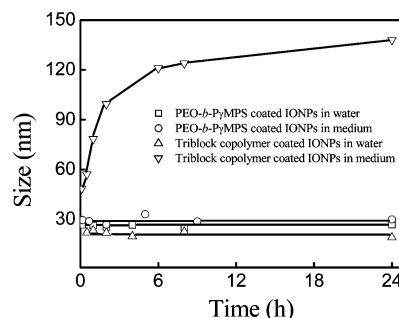


FIGURE 6. Hydrodynamic size of polysiloxane and amphiphilic copolymer-coated IONPs measured as a function of time upon incubation in distilled water and RPMI containing 10% FBS.

(32–36), clustered nanoparticles were typically formed, not the monodispersed nanoparticles as obtained in this study.

Considering the potential biomedical application of IONPs as MRI contrast agents, we have tested the T_2 weighted imaging and T_2 relaxation time. Figure 5 shows the measurement of transverse T_2 relaxation rate, which is the inverse of relaxation time of IONPs with different coating polymers. For the same IONP core size, polysiloxane polymer (PEO-*b*-PyMPS) coated IONPs (13 nm core size) exhibit the same T_2 relaxivity ($r_2 = 98.6 \text{ mM}^{-1} \text{ s}^{-1}$) as that of 13 nm amphiphilic copolymer coated IONPs ($r_2 = 93.6 \text{ Fe mM}^{-1} \text{ s}^{-1}$) (38). This indicates that such thin polysiloxane coating layer has little effect on their magnetic and contrast enhancing properties.

To verify the stability of polysiloxane-coated IONPs under physiological conditions and a medium that contains various bioactive macromolecules, we monitored the DLS measured size changes after IONPs were incubated in cell culture RPMI medium containing 10% fetal bovine serum (FBS) as simulated plasma. As shown in Figure 6, the hydrodynamic size of polysiloxane coated IONPs slightly increased ~ 3 nm compared with the size of IONPs in distilled water but keep

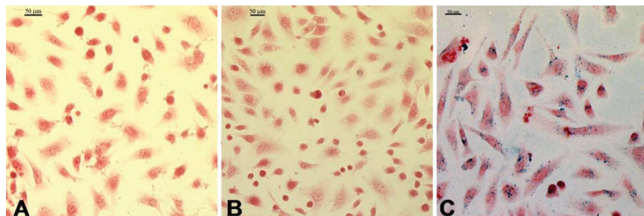


FIGURE 7. Images of Prussian blue staining of macrophage cell, RAW 264.7, after treatment with or without different IONPs samples at concentration of 0.2 mg/mL Fe: (a) control (without IONPs), (b) PEO-*b*-PyMPS coated IONPs, and (c) amphiphilic copolymer coated IONPs.

stable even after 24 h of incubation in RPMI 1640 medium containing 10 % serum. However, after being dispersed into culture medium, IONPs coated with amphiphilic copolymer (21, 37) begin to aggregate to large particles with diameter ~ 130 nm over 24 h incubation. The increase in hydrodynamic size may be attributed to the adsorption of plasma proteins in serum due to existence of carboxyl groups of amphiphilic copolymer used for coating IONPs.

One of the challenges in developing *in vivo* applications of nanoparticles is the nonspecific uptake of nanoparticles by the reticular endothelial system (RES) including liver and spleen, resulting in the functional nanoparticles being trapped by RES and unable to be secreted. Besides the concern of organ specific toxicity due to the accumulation of the nanoparticles, uptake by RES is a significant limitation in developing targeted imaging or delivery applications when it is preferred that nanoparticles can circulate long enough to be accumulated into the targeted area. Although it is considered that nanoparticles smaller than 50 nm are not easily recognized by cells of the RES, such as macrophages (39, 40), one strategy to reduce nonspecific uptake of nanoparticles by RES and macrophages is to control the properties of the polymer coating. To test if polysiloxane containing polymers may provide such capability, *in vitro* cell uptake experiments were carried out using a macrophage cell line. The uptake of PEO-*b*-PyMPS coated IONPs by macrophages was compared with that of commercially available conventional amphiphilic copolymers coated IONPs. Prussian blue staining for Fe was carried out to detect the presence of IONPs in cells, after 2 h of incubation of each IONP samples with macrophages. For amphiphilic polymer coated IONPs, substantial blue staining can be seen around the cell membrane as shown in Figure 7, suggesting a strong uptake of IONPs by macrophages. However, for PEO-*b*-PyMPS polymer coated IONPs, there was no blue staining observed in macrophages, indicating that there is no uptake of PEO-*b*-PyMPS coated IONPs by macrophages. This result clearly demonstrated that the polysiloxane coating layer drastically minimizes the recognition and phagocytosis of the composite nanoparticles by macrophages. Reduction of nonspecific cell uptakes of IONPs coated with polysiloxane based amphiphilic diblock copolymer reveals the antibiofouling effect of this new nanoparticle coating material.

CONCLUSION

Polysiloxane containing amphiphilic diblock copolymer poly(ethylene oxide)-*block*-poly(γ -methacryloxypropyl trimethoxysilane) (PEO-*b*-PyMPS) was developed to transform and stabilize magnetic iron oxide nanoparticles (IONPs) made in a hydrophobic medium in water. This class of amphiphilic diblock copolymer enables the stabilization and monodispersion of size uniformed hydrophobic IONPs in water. The copolymer can collapse onto the surface to form a polysiloxane layer with protection of PEO in water. This polysiloxane-coated IONPs show a strong effect in shortening transverse relaxation time T_2 and can be used for MRI contrast agent. Furthermore, such polysiloxane containing polymer exhibits antibiofouling property, which can reduce the interaction with macrophages and limit the intracellular uptake of IONPs by macrophages, and potentially minimize nonspecific uptake by RES in the future *in vivo* applications.

Acknowledgment. The authors thank Yunqiao Pu for GPC analyses. This work in part is supported by Emory-Georgia Tech Nanotechnology Center for Personalized and Predictive Oncology of NIH NCI Center of Cancer Nanotechnology Excellence (CCNE, U54 CA119338-01), Emory Molecular Translational Imaging Center of NIH *in vivo* Cellular and Molecular Imaging Center grant (ICMIC, P50CA128301-01A10003), and a research grant from EmTech Bio, Inc.

REFERENCES AND NOTES

- Berry, C. C.; Curtis, A. S. G. *J. Phys. D: Appl. Phys.* **2003**, *36*, R198–R206.
- Lee, H.; Lee, E.; Kim, D. K.; Jang, N. K.; Jeong, Y. Y.; Jon, S. *J. Am. Chem. Soc.* **2006**, *128*, 7383–7389.
- Xie, J.; Xu, C.; Kohler, N.; Hou, Y.; Sun, S. *Adv. Mater.* **2007**, *19*, 3163+.
- Lee, H.; Yu, M. K.; Park, S.; Moon, S.; Min, J. J.; Jeong, Y. Y.; Kang, H. W.; Jon, S. *J. Am. Chem. Soc.* **2007**, *129*, 12739–12745.
- Jun, Y. W.; Huh, Y. M.; Choi, J. S.; Lee, J. H.; Song, H. T.; Kim, S.; Yoon, S.; Kim, K. S.; Shin, J. S.; Suh, J. S.; Cheon, J. *J. Am. Chem. Soc.* **2005**, *127*, 5732–5733.
- Xie, J.; Xu, C. J.; Xu, Z. C.; Hou, Y. L.; Young, K. L.; Wang, S. X.; Pourmond, N.; Sun, S. H. *Chem. Mater.* **2006**, *18*, 5401–5403.
- Lu, C. W.; Hung, Y.; Hsiao, J. K.; Yao, M.; Chung, T. H.; Lin, Y. S.; Wu, S. H.; Hsu, S. C.; Liu, H. M.; Mou, C. Y.; Yang, C. S.; Huang, D. M.; Chen, Y. C. *Nano Lett.* **2007**, *7*, 149–154.
- Morel, A. L.; Nikitenko, S. I.; Gionnet, K.; Wattiaux, A.; Lai-Kee-Him, J.; Labrugere, C.; Chevalier, B.; Deleris, G.; Petitbois, C.; Brisson, A.; Simonoff, M. *ACS Nano* **2008**, *2*, 847–856.
- Piao, Y.; Burns, A.; Kim, J.; Wiesner, U.; Hyeon, T. *Adv. Funct. Mater.* **2008**, *18*, 3745–3758.
- Jeong, U.; Teng, X. W.; Wang, Y.; Yang, H.; Xia, Y. N. *Adv. Mater.* **2007**, *19*, 33–60.
- Bruce, I. J.; Taylor, J.; Todd, M.; Davies, M. J.; Borioni, E.; Sangregorio, C.; Sen, T. *J. Magn. Magn. Mater.* **2004**, *284*, 145–160.
- Stober, W.; Fink, A.; Bohn, E. *J. Colloid Interface Sci.* **1968**, *26*, 62–68.
- Yi, D. K.; Selvan, S. T.; Lee, S. S.; Papaefthymiou, G. C.; Kundaliya, D.; Ying, J. Y. *J. Am. Chem. Soc.* **2005**, *127*, 4990–4991.
- Philipse, A. P.; Vanbruggen, M. P. B.; Pathmamanoharan, C. *Langmuir* **1994**, *10*, 92–99.
- Lu, Y.; Yin, Y. D.; Mayers, B. T.; Xia, Y. N. *Nano Lett.* **2002**, *2*, 183–186.
- Sun, Y. K.; Duan, L.; Guo, Z. R.; Yun, D. M.; Ma, M.; Xu, L.; Zhang, Y.; Gu, N. *J. Magn. Mater.* **2005**, *285*, 65–70.
- Santra, S.; Tapeç, R.; Theodoropoulou, N.; Dobson, J.; Hebard, A.; Tan, W. H. *Langmuir* **2001**, *17*, 2900–2906.

- (18) De Palma, R.; Peeters, S.; Van Bael, M. J.; Van den Rul, H.; Bonroy, K.; Laureyn, W.; Mullens, J.; Borghs, G.; Maes, G. *Chem. Mater.* **2007**, *19*, 1821–1831.
- (19) Li, Y. T.; Lokitz, B. S.; McCormick, C. L. *Macromolecules* **2006**, *39*, 81–89.
- (20) Yu, W. W.; Falkner, J. C.; Yavuz, C. T.; Colvin, V. L. *Chem. Commun.* **2004**, *20*, 2306–2307.
- (21) Gao, X. H.; Cui, Y. Y.; Levenson, R. M.; Chung, L. W. K.; Nie, S. M. *Nat. Biotechnol.* **2004**, *22*, 969–976.
- (22) Luo, S. Z.; Xu, J.; Zhang, Y. F.; Liu, S. Y.; Wu, C. J. *J. Phys. Chem. B* **2005**, *109*, 22159–22166.
- (23) Mellon, W.; Rinaldi, D.; Bourgeat-Lami, E.; D'Agosto, F. *Macromolecules* **2005**, *38*, 1591–1598.
- (24) Zhang, Y. F.; Luo, S. Z.; Liu, S. Y. *Macromolecules* **2005**, *38*, 9813–9820.
- (25) Du, J. Z.; Chen, Y. M. *Macromolecules* **2004**, *37*, 6322–6328.
- (26) Chen, Y. M.; Du, J. Z.; Xiong, M.; Zhang, K.; Zhu, H. *Macromol. Rapid Commun.* **2006**, *27*, 741–750.
- (27) Du, J. Z.; Chen, Y. M. *Macromol. Rapid Commun.* **2005**, *26*, 491–494.
- (28) Zhang, C. F.; Jugold, M.; Woenne, E. C.; Lammers, T.; Morgenstern, B.; Mueller, M. M.; Zentgraf, H.; Bock, M.; Eisenhut, M.; Semmler, W.; Kiessling, F. *Cancer Res.* **2007**, *67*, 1555–1562.
- (29) Ma, D. L.; Veres, T.; Clim, L.; Normandin, F.; Guan, J. W.; Kingston, D.; Simard, B. *J. Phys. Chem. C* **2007**, *111*, 1999–2007.
- (30) Gindy, M. E.; Panagiotopoulos, A. Z.; Prud'homme, R. K. *Langmuir* **2008**, *24*, 83–90.
- (31) Zhang, L.; Lin, J.; Lin, S. *Macromolecules* **2007**, *40*, 5582–5592.
- (32) Ai, H.; Flask, C.; Weinberg, B.; Shuai, X.; Pagel, M. D.; Farrell, D.; Duerk, J.; Gao, J. M. *Adv. Mater.* **2005**, *17*, 1949+.
- (33) Nasongkla, N.; Bey, E.; Ren, J. M.; Ai, H.; Khemtong, C.; Guthi, J. S.; Chin, S. F.; Sherry, A. D.; Boothman, D. A.; Gao, J. M. *Nano Lett.* **2006**, *6*, 2427–2430.
- (34) Kim, B. S.; Qiu, J. M.; Wang, J. P.; Taton, T. A. *Nano Lett.* **2005**, *5* (10), 1987–1991.
- (35) Kim, B. S.; Taton, T. A. *Langmuir* **2007**, *23*, 2198–2202.
- (36) Euliss, L. E.; Grancharov, S. G.; O'Brien, S.; Deming, T. J.; Stucky, G. D.; Murray, C. B.; Held, G. A. *Nano Lett.* **2003**, *3*, 1489–1493.
- (37) Gao, X. H.; Yang, L. L.; Petros, J. A.; Marshal, F. F.; Simons, J. W.; Nie, S. M. *Curr. Opin. Biotechnol.* **2005**, *16*, 63–72.
- (38) Duan, H. W.; Kuang, M.; Wang, X. X.; Wang, Y. A.; Mao, H.; Nie, S. M. *J. Phys. Chem. C* **2008**, *112*, 8127–8131.
- (39) Rogers, W. J.; Basu, P. *Atherosclerosis* **2005**, *178*, 67–73.
- (40) Raynal, I.; Prigent, P.; Peyramaure, S.; Najid, A.; Rebuzzi, C.; Corot, C. *Invest. Radiol.* **2004**, *39*, 56–63.

AM900262J